Large Bandwidth and High Accuracy Photonic-Assisted Instantaneous Microwave Frequency Estimation System based on an Integrated Silicon Micro-Resonator

Haifeng Shao [1, 2], Hui Yu [1], Xiaoqing Jiang [1], Jianyi Yang [1], Gunther Roelkens [2]
[1] Integrated Optics Lab, ISEE, Zhejiang University, Hang Zhou, China
[2] Photonics Research Group, INTEC, Ghent University, B-9000 Ghent, Belgium
Email: iseejxq@zju.edu.cn

***Abstract*—We demonstrate two instantaneous frequency measurement systems based on silicon photonics. One has a large bandwidth from 0.5 GHz to 35 GHz, while the other one exhibits a small RMS error of 63 MHz.**

Keywords—instantaneous frequency measurement, large bandwidth, high accuracy, silicon photonics

I. INTRODUCTION

A photonic-assisted instantaneous frequency measurement (IFM) system with large bandwidth, high accuracy is extremely desirable in modern radar warning equipment. The basic principle behind this photonic technique is to map the unknown microwave frequency to an optical power ratio, which is referred as the amplitude comparison function (ACF). Most reported IFM systems were [1, 2, 3] built with discrete optoelectronic components and are bulky and expensive. Therefore an integrated IFM system [4] is considered as an effective solution to address this issue. Until now, integrated IFM systems have been implemented on different material platforms including Si_3N_4 [5] and InP [6]. However in [5] the system bandwidth is only 3 GHz which is limited by the large radius of Si_3N_4 micro-ring resonator. Moreover the need for high-speed power detection and an EDFA increases the cost of the system. In [6] measurement ambiguities exist around 5 GHz and 15 GHz since ACF is not a monotonous function. In this paper, we propose and demonstrate an IFM scheme with large bandwidth and high accuracy on the silicon-on-insulator (SOI) platform. It consists of a Mach-Zehnder modulator (MZM) and an add-drop micro-ring filter. By exploiting the two complementary outputs from the through and the drop ports of an add-drop ring, we obtain a broadband, steep and monotonous ACF (over the whole frequency range) based on which two IFM systems are demonstrated. One has a large bandwidth from 0.5 GHz to 35 GHz, while the other one of high accuracy exhibits a root mean square (RMS) frequency error of 63 MHz.

II. PRINCIPLE OF OPERATION AND EXPERIMENTAL SET-UP

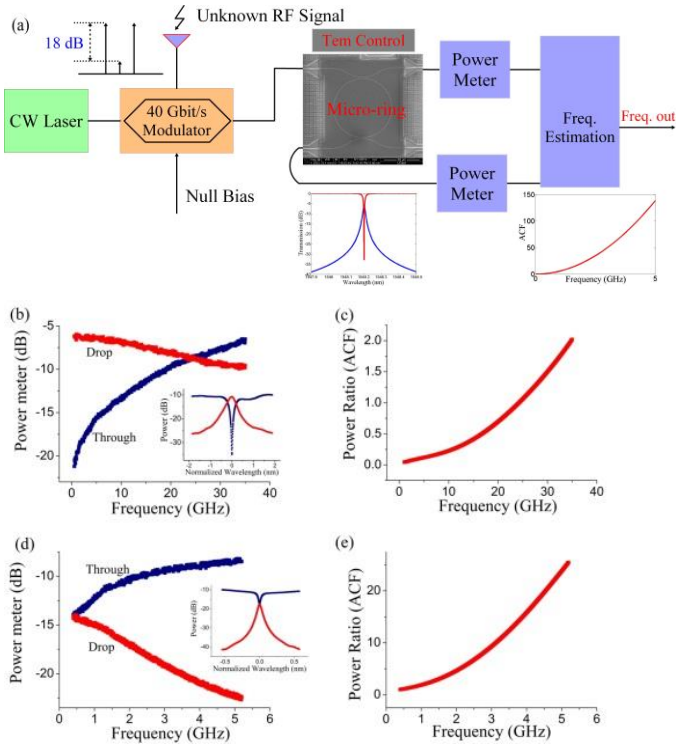

Fig. 1. (a) Schematic diagram of the IFM system, (b)-(e) Measured output powers from the through and drop ports of the ring, and their ratio (ACF) versus the RF frequency. The two insets display the transmission spectra. (b) and (c) are for the large bandwidth IFM system, (d) and (e) are for the high accuracy IFM system.

Figure 1(a) shows the experimental IFM system which consists of a MZM that works at the double-sideband suppressed-carrier operation point [6] and an add-drop micro-ring filter. An optical carrier (Santec tunable laser, 10 mW) which matches the resonance wavelength of the micro-ring is launched into a 40 Gbit/s Mach-Zehnder modulator (MZM), which is modulated by an unknown RF signal from a Rohde & Schwarz R40 RF signal generator. The MZM is biased at the minimum transmission point to eliminate all the even-order harmonics. In the small signal regime, the higher odd-order sidebands can be

neglected and only two first-order sidebands left. The sideband-to-carrier ratio is 18 dB as shown in Fig. 1(a). The modulated beam is then coupled into the chip by a fiber-to-chip-grating coupler. The rib waveguide forming the ring has a cross section of 500×220 nm^2 and a slab thickness of 150 nm. The 25-μm-radius leads to a FSR around 4nm. The ratio of the power at the through port to that of the drop port depends on the location of the two sidebands and thus the RF frequency. The simulation result in Fig. 1(a) shows the ACF curve of a critical coupled ring. To determine the RF frequency, the characteristic ACF curve of the IFM system is first characterized with a RF signal whose frequency is already known. With it as a reference, we can easily get the frequency of the RF signal under test by measuring the power ratio between the through and the drop ports. The temperature is stabilized at 20 °C to avoid a resonance frequency shift during the measurement. Figures 1(b) and (d) display the output power at the through and the drop ports as a function of the RF frequency for two add-drop rings. The corresponding characteristic ACF curves of the systems are presented in Fig. 1(c) and Fig. 1(e). The ring in Fig. 1(b) and (c) with a gap of 300nm (Q=3974) between the ring and bus waveguide is designed to achieve a large bandwidth, while the other in Fig. 1(d) and (e) with a gap of 700 nm (Q=25833) is to achieve a high accuracy. The total insertion loss is about 10 dB.

To verify the system's performance, different RF input power levels are applied. The signal frequency is swept from 0.5 to 35 GHz (in steps of 0.1 GHz) and 0.5-5GHz (in steps of 0.02 GHz) for the large bandwidth and the high accuracy IFM systems, respectively. After post-processing, we get the ACF of the signal undertest and compare it with the reference in Fig. 1 (c) and (e) to extract the frequency information.

III. RESULTS

The measured frequency error (fmeasure-finput) as a function of RF frequency is shown in Fig. 2. For the large bandwidth IFM system (35 GHz), most errors of different RF input power levels (10 dBm-4 dBm) occur below 600 MHz, the corresponding RMS error is about 240 MHz.

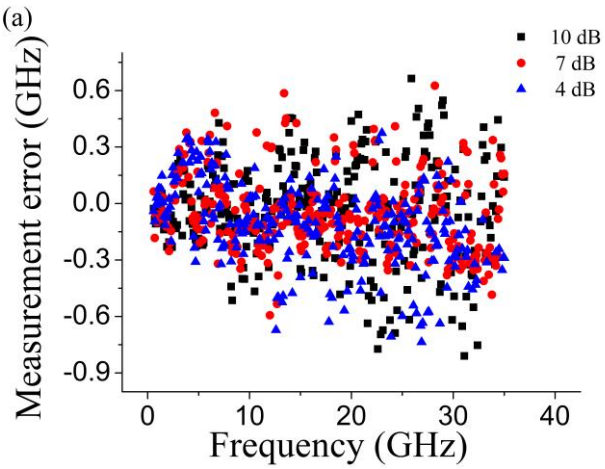

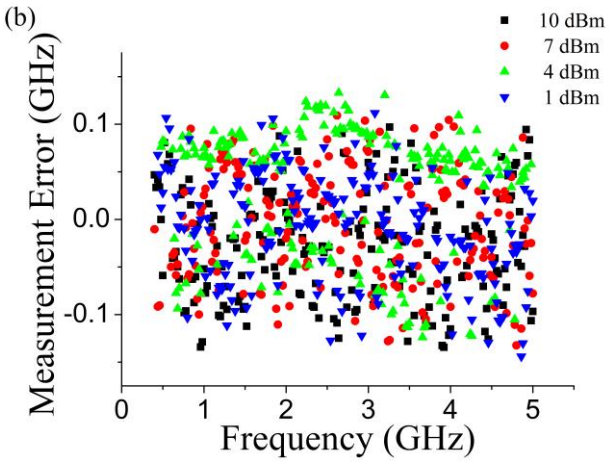

Fig. 2. Measured frequency error as the function of RF signal frequency in (a) Large range IFM system (b) High accuracy IFM system

For the high accuracy IFM system, the RMS frequency error is 63 MHz within the frequency range from 0.5 GHz to 5 GHz.

IV. CONCLUTION

We have experimentally demonstrated two IFM systems with large bandwidth (0.5-35 GHz) and high accuracy (RMS=63 MHz) respectively. If properly designed, the systems have a wideband and monotonous ACF. The system performance could be further improved by designing a critically coupling ring and integrating all active and passive components in a single silicon chip.

ACKNOWLEDGMENT

This work is supported by the Nature Basic Research Program of China (2013CB632105), the National Natural Science Foundations of China (61177055 and 61307074), the Fundamental Research Funds for the Central Universities and China Scholarship Council.

REFERENCES

[1] X. Zou et al., "Microwave frequency measurement based on optical power monitoring using a complementary optical filter pair," IEEE Trans. Microwave Theor. Tech. vol. 57(2), pp. 505-511, Feb. 2009.

[2] M. V. Drummond et al., "Photonic RF instantaneous frequency measurement system by means of a polarization-domain interferometer," Opt. Express, vol. 17(7), pp. 5433-5438, 2009.

[3] L. A. Bui et al., "Remoted all optical instantaneous frequency measumement system using nonlinear mixing in highly nonlinear optical fiber", Opt. Express, vol. 21(7), pp. 8550-8557, 2013

[4] D. Marpaung et al., "Integrated microwave photonics," Laser Photon. Rev. vol. 7(4), pp. 506-538, 2013.

[5] D. Marpaung, "On-chip photonic-assisted instantaneous microwave frequency measurement system," IEEE Photon. Technol. Lett., vol. 25 (9), pp. 837-840, 2013.

[6] J. S. Fandino et al., "Photonics-based microwave frequency measurement using a double-sideband suppressed-carrier modulation and an InP integrated ring-assisted Mach-Zehnder interferometer filter," Opt. Lett., vol. 38 (21), pp. 4316-4319, 2013.